Subgrid-scale backscatter in turbulent and transitional flows

Ugo Piomelli, William H. Cabot, Parviz Moin, and Sangsan Lee

Citation: Physics of Fluids A: Fluid Dynamics **3**, 1766 (1991);
View online: https://doi.org/10.1063/1.857956
View Table of Contents: http://aip.scitation.org/toc/pfa/3/7
Published by the American Institute of Physics

Subgrid-scale backscatter in turbulent and transitional flows

Ugo Piomelli,[a] William H. Cabot, Parviz Moin, and Sangsan Lee
Center for Turbulence Research, Stanford, California 94305

(Received 29 October 1990; accepted 7 March 1991)

Most subgrid-scale (SGS) models for large-eddy simulations (LES) are absolutely dissipative (that is, they remove energy from the large scales at each point in the physical space). The actual SGS stresses, however, may transfer energy to the large scales (backscatter) at a given location. Recent work on the LES of transitional flows [Piomelli *et al.*, Phys. Fluids A **2**, 257 (1990)] has shown that failure to account for this phenomenon can cause inaccurate prediction of the growth of the perturbations. Direct numerical simulations of transitional and turbulent channel flow and compressible isotropic turbulence are used to study the backscatter phenomenon. In all flows considered roughly 50% of the grid points were experiencing backscatter when a Fourier cutoff filter was used. The backscatter fraction was less with a Gaussian filter, and intermediate with a box filter in physical space. Moreover, the backscatter and forward scatter contributions to the SGS dissipation were comparable, and each was often much larger than the total SGS dissipation. The SGS dissipation (normalized by total dissipation) increased with filter width almost independently of filter type. The amount of backscatter showed an increasing trend with Reynolds number. In the near-wall region of the channel, events characterized by strong Reynolds shear stress correlated fairly well with areas of high SGS dissipation (both forward and backward). In compressible isotropic turbulence similar results were obtained, independent of fluctuation Mach number.

I. INTRODUCTION

Large-eddy simulation (LES) is based on the assumption that the modeled small scales are nearly homogeneous and isotropic. Most of the commonly used subgrid-scale (SGS) models, moreover, assume that the main function of subgrid scales is to remove energy from the large scales and dissipate it through the action of the viscous forces. It has been known for some years, however, that while, on average, energy is transferred from the large to the small scales ("forward scatter"), reversed energy flow ("backscatter") from the small scales to the large ones may also occur intermittently.

The most commonly used subgrid-scale stress model, the Smagorinsky model,[1] is absolutely dissipative, i.e., can only account for forward scatter. This model has been reasonably successful in simulations of simple turbulent flows; its success is probably due to its ability to predict the global energy drain by the small scales even if the details of the model are incorrect.[2]

Very few of the SGS models used in the past are capable of providing backscatter. The mixed model,[3] for example, has a part that is not absolutely dissipative, the scale-similar part; in channel flow this term provides backscatter.[4]

Recent work on the LES of transitional flows[5] has shown that during the early nonlinear stages of transition energy is transferred from small scales to large scales even in the mean, and that failure to account for this phenomenon can cause inaccurate prediction of the growth of the perturbations. The use of the Smagorinsky model led to the decay of the perturbations even in instances in which the flow should have been unstable. Acceptable results were obtained, however, by introducing an intermittency factor which turned off the eddy viscosity model until the perturbations had grown to finite amplitudes and had altered the mean velocity profile. A model based on the renormalization group (RNG) theory of Yakhot and Orszag[6] was also used by Piomelli *et al.*[7] This model, although essentially dissipative and thus unable to predict backscatter, gave zero eddy viscosity at the early stages of transition, and allowed fairly accurate prediction of transition in a flat-plate boundary layer. The model, however, was found to depend strongly on the length scale used.

Leith[8] proposed an SGS stress model including a stochastic backscatter force designed to yield a k^4 energy spectrum (k is the wave number); this model was used for the LES of a two-dimensional mixing layer. Although his results show the correct growth rate of the layer, no comparison is made with calculations in which the stochastic force is omitted.

Chasnov[9] presented an SGS stress model that includes a stochastic backscatter force based on the eddy-damped quasinormal Markovian (EDQNM) model. Use of this model in a LES computation of freely decaying isotropic turbulence gave results in good agreement with theoretical predictions. By contrast, use of an eddy viscosity model did not yield the expected spectral decay in the inertial subrange.

Recently, Germano *et al.*[10] also proposed a model which can provide backscatter. They applied this model to the simulation of transitional and turbulent channel flow and obtained results in good agreement with the direct simulations.

On the basis of the studies mentioned above, the accurate modeling of backscatter appears desirable, especially for nonequilibrium flows. Although backscatter modeling has recently received some attention, little effort has actually been made to quantify this phenomenon, especially in wall-bounded flows. In this study, the velocity fields obtained

[a] Permanent address: Department of Mechanical Engineering, University of Maryland, College Park, Maryland 20742.

 0899-8213/91/071766-06$02.00

from direct numerical simulations (DNS) of the Navier–Stokes equations will be used to calculate subgrid-scale dissipation and backscatter. Although this work will concentrate on transitional and turbulent plane channel flows, compressible homogeneous isotropic turbulence has also been examined. In the next section the equations relevant to the problem will be presented; in Sec. III results of *a priori* tests performed on the numerical simulations will be discussed. Finally, in Sec. IV conclusions will be drawn.

II. MATHEMATICAL FORMULATION

In large-eddy simulation the large-scale quantities (indicated by an overbar) are defined by the filtering operation

$$\bar{f}(\mathbf{x}) = \int f(\mathbf{x}')G(\mathbf{x},\mathbf{x}')d\mathbf{x}', \tag{1}$$

in which G is the filter function and the integral is extended to the entire domain. Applying the filtering operation to the Navier–Stokes equations yields the dimensionless filtered continuity and Navier–Stokes equations

$$\frac{\partial \bar{u}_i}{\partial x_i} = 0, \tag{2}$$

$$\frac{\partial \bar{u}_i}{\partial t} + \frac{\partial}{\partial x_j}(\bar{u}_i\bar{u}_j) = -\frac{\partial \bar{p}}{\partial x_i} - \frac{\partial \tau_{ij}}{\partial x_j} + \frac{1}{\mathrm{Re}}\frac{\partial^2 \bar{u}_i}{\partial x_j\,\partial x_j}. \tag{3}$$

Equations (2) and (3) govern the evolution of the large scales. The effects of the small scales appear in the SGS stress

$$\tau_{ij} = \overline{u_i u_j} - \bar{u}_i\bar{u}_j, \tag{4}$$

which must be modeled.

To examine the effect of the SGS stress model on the resolved scales, consider the transport equation for the resolved energy $\bar{q}^2 = \bar{u}_i\bar{u}_i$

$$\frac{\partial \bar{q}^2}{\partial t} + \frac{\partial}{\partial x_j}(\bar{q}^2\bar{u}_j) = \frac{\partial}{\partial x_j}\left(-2\bar{p}\bar{u}_j - 2\bar{u}_i\tau_{ij} + \frac{1}{\mathrm{Re}}\frac{\partial \bar{q}^2}{\partial x_j}\right) - \frac{2}{\mathrm{Re}}\frac{\partial \bar{u}_i}{\partial x_j}\frac{\partial \bar{u}_i}{\partial x_j} + 2\tau_{ij}\bar{S}_{ij}, \tag{5}$$

in which $\bar{S}_{ij}$ is the large-scale strain-rate tensor

$$\bar{S}_{ij} = \frac{1}{2}\left(\frac{\partial \bar{u}_i}{\partial x_j} + \frac{\partial \bar{u}_j}{\partial x_i}\right). \tag{6}$$

One-half of the last term on the right-hand side of (5) will be referred to as the "subgrid-scale dissipation," $\epsilon_{\mathrm{SGS}} = \tau_{ij}\bar{S}_{ij}$; it represents the energy transfer between resolved and subgrid scales. If it is negative, the subgrid scales remove energy from the resolved ones (forward scatter); if it is positive, they release energy to the resolved scales (backscatter). The backward and forward scatter components of ϵ_{SGS}, respectively, denoted by ϵ_+ and ϵ_-, are defined as

$$\epsilon_+ = \tfrac{1}{2}(\epsilon_{\mathrm{SGS}} + |\epsilon_{\mathrm{SGS}}|), \quad \epsilon_- = \tfrac{1}{2}(\epsilon_{\mathrm{SGS}} - |\epsilon_{\mathrm{SGS}}|). \tag{7}$$

It is easy to see that eddy viscosity SGS stress models of the Smagorinsky type are absolutely dissipative, since they assume that the eddy viscosity ν_T is positive, which gives

$$\tau_{ij}\bar{S}_{ij} = -2\nu_T\bar{S}_{ij}\bar{S}_{ij} < 0. \tag{8}$$

To investigate the character of backscatter in turbulent flows the velocity fields obtained from the direct numerical simulation (DNS) of the Navier–Stokes equations were filtered to yield the exact resolved and subgrid-scale velocities, and the exact subgrid-scale dissipation. The filter functions used in this work are the Gaussian filter, the box filter in physical space, and the sharp cutoff filter. The Gaussian filter is given by

$$G_i(x_i,x_i') = (6/\pi\Delta_i)^{1/2}\exp[6(x_i - x_i')^2/\Delta_i^2], \tag{9}$$

the box filter is defined as

$$G_i(x_i,x_i') = \begin{cases} 1/\Delta_i, & \text{for } |x_i - x_i'| < \Delta_i/2, \\ 0, & \text{otherwise,} \end{cases} \tag{10}$$

while the cutoff filter is most conveniently defined in Fourier space:

$$\hat{G}_i(k_i) = \begin{cases} 1, & \text{for } k_i \leqslant K_i, \\ 0, & \text{otherwise,} \end{cases} \tag{11}$$

where $\hat{G}_i$ is the Fourier coefficient of the filter function in the ith direction, G_i, $K_i = \pi/\Delta_i$ is the cutoff wave number, and Δ_i is the filter width in the ith direction.

III. RESULTS AND DISCUSSION

The direct simulation results used for the study of backscatter in channel flows were those of Kim *et al.*[11] for turbulent channel flow, and those of Zang *et al.*[12] for the temporally developing transitional channel flow. In all cases x or x_1 is the streamwise direction, y or x_2 is the direction normal to the walls, which are located at $y = \pm 1$, and z or x_3 is the spanwise direction; u, v and w are the velocity components along the coordinate directions. Reynolds numbers are $\mathrm{Re} = 3300$ and 7900 (based on centerline velocity U_c and channel half-width) for the turbulent case and $\mathrm{Re} = 8000$ for the transitional case (based on the initial laminar centerline velocity and channel half-width). The $\mathrm{Re} = 7900$ turbulent flow DNS was performed after the publication of Ref. 11; the same numerical method used for the lower Reynolds number case was employed, and $256\times193\times192$ grid points were used to give the same resolution, in wall units, as in the lower Reynolds number simulation.

In Fig. 1 the plane-averaged and root-mean-square subgrid-scale dissipation are shown for the $\mathrm{Re} = 3300$ case. In the following, $\langle\ \rangle$ indicates averaging over a plane parallel to the wall, while $\langle\ \rangle_V$ indicates averaging over the entire computational domain. To increase the sample size, the results were averaged over several flow realizations and over both sides of the channel, whenever possible. The SGS dissipation and backscatter will be normalized by either the volume- or plane-averaged *absolute value* of the viscous dissipation, defined as

$$\epsilon_v = |-(2/\mathrm{Re})S_{ij}S_{ij}|, \tag{12}$$

where

$$S_{ij} = \frac{1}{2}\left(\frac{\partial u_i}{\partial x_j} + \frac{\partial u_j}{\partial x_i}\right). \tag{13}$$

The amount of filtering will be characterized by α, the ratio of subgrid-scale kinetic energy $\langle q_{\mathrm{SGS}}^2\rangle_V$ (where $q_{\mathrm{SGS}}^2 = \tau_{ii}$) to total turbulent kinetic energy $\langle q^2\rangle_V$. Since filtering was only applied in the planes parallel to the wall, the ratio of the

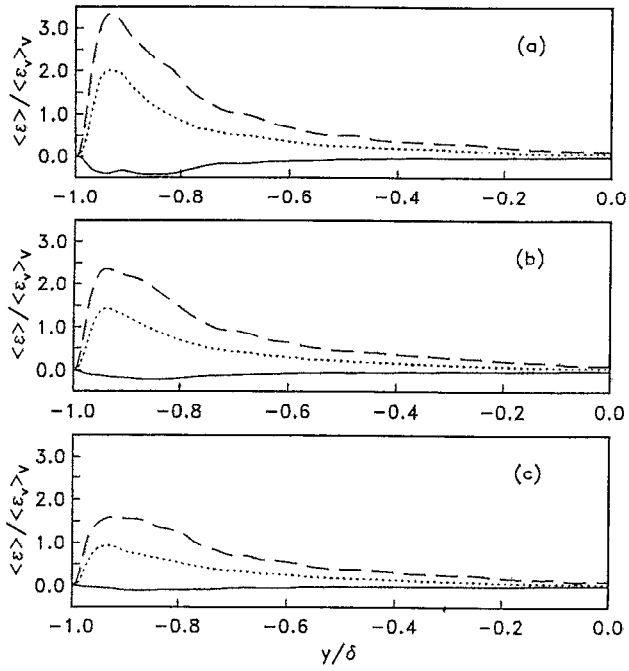

FIG. 1. Subgrid-scale dissipation normalized by $\langle\epsilon_v\rangle_v$; Re = 3300 turbulent channel flow, cutoff filter. ——: Plane-averaged dissipation $\langle\epsilon_{SGS}\rangle$; – – –: root-mean-square fluctuation of ϵ_{SGS}; ····: plane-averaged backscatter $\langle\epsilon_+\rangle$. (a) $\Delta_i = 4\Delta x_i$, $\alpha = 0.10$; (b) $\Delta_i = 8\Delta x_i/3$, $\alpha = 0.04$; (c) $\Delta_i = 2\Delta x_i$, $\alpha = 0.02$.

filter width Δ_i to the grid size Δx_i reported here refers to the streamwise and spanwise directions.

Figure 1 indicates that the backscatter contribution to ϵ_{SGS} is much larger than the mean for all filter widths examined. While the subgrid scales extract energy from the large scales in the mean, large values of ϵ_+ and ϵ_- can be expected. The fraction of points in each plane that experience backscatter (shown in Fig. 2) is close to 50%, almost independent of filter width and distance from the wall. This result was found to hold for all flows examined, including the transitional channel flow and the compressible isotropic decay.

Both backward and forward scatter peak in the near-wall region, at approximately $y^+ = 12$ (variables indicated by a superscript + are normalized by the kinematic viscosity ν and the friction velocity u_τ). In the near-wall region of the channel, events characterized by strong Reynolds shear

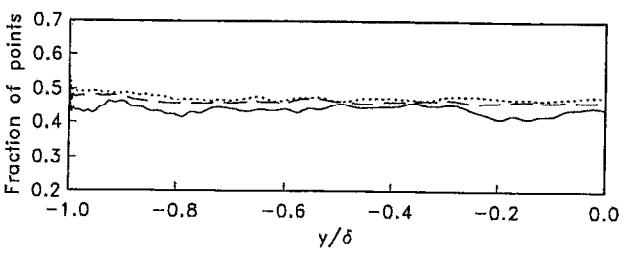

FIG. 2. Fraction of grid points where $\epsilon_{SGS} > 0$; Re = 3300 turbulent channel flow, cutoff filter. ——: $\Delta_i = 4\Delta x_i$, $\alpha = 0.10$; – – –: $\Delta_i = 8\Delta x_i/3$, $\alpha = 0.04$; ····: $\Delta_i = 2\Delta x_i$, $\alpha = 0.02$.

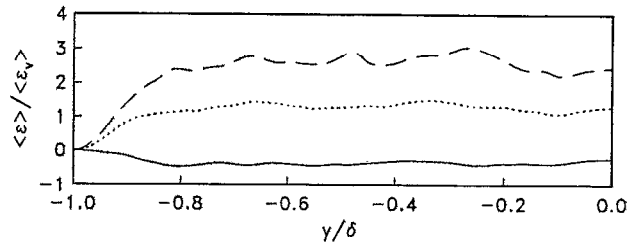

FIG. 3. Subgrid-scale dissipation normalized by $\langle\epsilon_v\rangle$; Re = 3300 turbulent channel flow, $\Delta_i = 4\Delta x_i$, $\alpha = 0.10$; cutoff filter. ——: Plane-averaged dissipation $\langle\epsilon_{SGS}\rangle$; – – –: root-mean-square fluctuation of ϵ_{SGS}; ····: plane-averaged backscatter $\langle\epsilon_+\rangle$.

stress correlate fairly well with areas of high SGS dissipation (both forward and backward). The unconditioned correlation coefficient between ϵ_{SGS} and uv is only 0.28 at $y^+ = 7$, but decays to nearly zero above $y^+ = 15$. This value increases to 0.45 at $y^+ = 7$ if the correlation coefficient is conditioned on the absolute value of uv being larger than its rms. Comparison of contours of uv and of ϵ_{SGS} at various x-z planes confirmed this conclusion. The subgrid-scale dissipation normalized by the plane-averaged viscous dissipation (Fig. 3) increases with distance from the wall and levels off at about one-quarter of the channel half-width, where its rms is almost three times the viscous dissipation.

Similar results were obtained from the Re = 7900 channel flow (compare Figs. 1 and 4). In the transitional cases examined (Fig. 5), however, significant differences were observed. First, at the early stages of transition (for $t < 180$) backscatter was found to occur in the mean in the near-wall region.[5] At these stages, furthermore, both ϵ_{SGS} and ϵ_+ peaked much farther from the wall than in turbulent flow, near the critical layer of the initial disturbances. As the flow goes through transition, small scales are generated in the near-wall region, and the location of maximum ϵ_{SGS} moves toward the wall. High values of SGS dissipation and backscatter are, however, still observed away from the wall throughout the transition process.

When the Gaussian filter was used the magnitude of ϵ_+ was significantly reduced over that found using the cutoff filter (Fig. 6), although backscatter still occurred at approximately 30% of the grid points. In practice, the Gaussian filter is usually coupled with a sharp cutoff filter, so that the subgrid-scale velocity has a contribution from the small

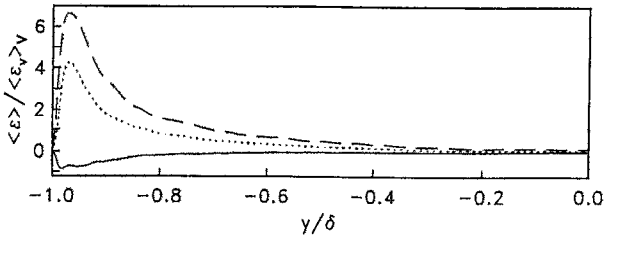

FIG. 4. Subgrid-scale dissipation normalized by $\langle\epsilon_v\rangle_v$; Re = 7900 turbulent channel flow, $\Delta_i = 4\Delta x_i$, $\alpha = 0.04$; cutoff filter. ——: Plane-averaged dissipation $\langle\epsilon_{SGS}\rangle$; – – –: root-mean-square fluctuation of ϵ_{SGS}; ····: plane-averaged backscatter $\langle\epsilon_+\rangle$.

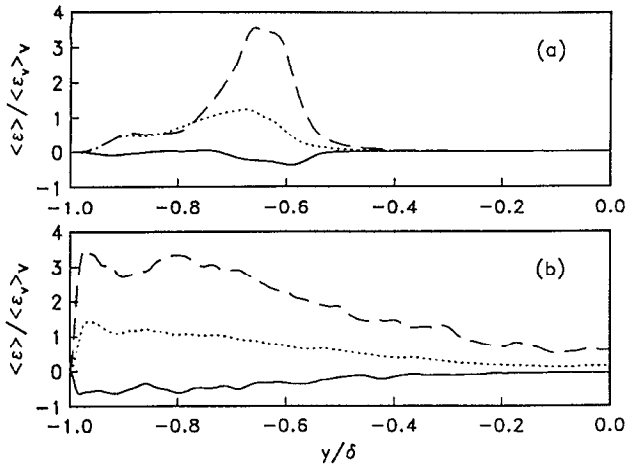

FIG. 5. Subgrid-scale dissipation normalized by $\langle\epsilon_v\rangle_V$; Re = 8000 transitional channel flow, cutoff filter. ——: Plane-averaged dissipation $\langle\epsilon_{SGS}\rangle$; – – –: root-mean-square fluctuation of ϵ_{SGS}; ····: plane-averaged backscatter $\langle\epsilon_+\rangle$. (a) $\Delta_i = 8\Delta x_i$, $\alpha = 0.01$, $t = 170$; (b) $\Delta_i = 4\Delta x_i$, $\alpha = 0.03$, $t = 200$.

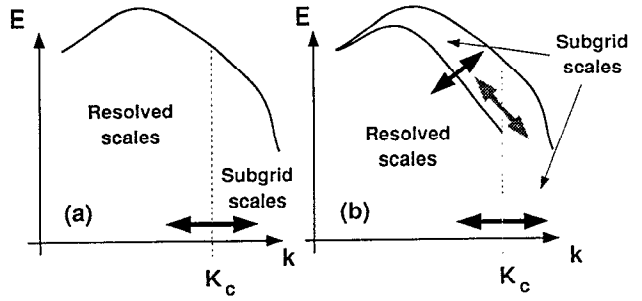

FIG. 7. Sketch of the interactions between large and small scales in spectral space. (a) Cutoff filter; (b) Gaussian filter.

scales (those beyond the cutoff) and one from the scales resolved on the grid. The subgrid-scale dissipation, therefore, accounts for part of the energy transferred between the scales above the cutoff, and a portion of the energy transferred between scales above the cutoff and those below it (the interaction indicated by the dark arrows in Fig. 7). Another portion of the energy transferred by this interaction (indicated by the lighter arrow), however, appears as an energy transfer between the subgrid scales in the transport equation for q^2_{SGS} with the Gaussian filter, whereas it contributes to the backscatter with the cutoff filter. When the box filter is used the SGS dissipation and backscatter are intermediate between those obtained with the Gaussian and the cutoff filters (Fig. 8).

The volume-averaged subgrid-scale dissipation and fraction of backscatter points for the turbulent channel flows examined are shown in Fig. 9. The volume-averaged viscous dissipation $\langle\epsilon_v\rangle_V$ is equal to 14.8 and 15.8 (normalized by u_τ, ν, and δ), respectively, for the Re = 3300 and Re = 7900 cases. The SGS dissipation (normalized by total dissipation) increased with filter width almost independently of filter type and Reynolds number. The amount of backscatter (Fig. 10) appears to slightly increase with Reynolds number, a trend confirmed by the finding that $\langle\epsilon_+\rangle/\langle\epsilon_v\rangle$ also increases with distance from the wall (see Fig. 3).

The results obtained from the compressible isotropic decay simulations exhibit the same trends observed above. The direct simulation data were taken from the results of Lee *et al.*[13] For the compressible flow simulations the subgrid-scale stresses τ_{ij} and dissipation ϵ_{SGS}, and the viscous dissipation ϵ_v are defined as

$$\tau_{ij} = \bar{\rho}(\widetilde{u_i u_j} - \tilde{u}_i\tilde{u}_j), \tag{14}$$

$$\epsilon_{SGS} = \tau_{ij}\tilde{S}_{ij}, \tag{15}$$

$$\epsilon_v = \frac{4}{3}\bar{\mu}\,\overline{\left(\frac{\partial u_i}{\partial x_i}\right)^2} + \bar{\mu}\,\overline{\omega_i\omega_i}, \tag{16}$$

where the tilde denotes Favre filtering, and ω_i is the ith component of the vorticity vector $\omega_i = \epsilon_{ijk}\,\partial u_k/\partial x_j$ (in which ϵ_{ijk} is the alternating tensor). Although (16) is exact only if the viscosity is constant, variable viscosity effects were found to be negligible within the range of parameters examined here.[13] The results from three simulations were examined with initial turbulent fluctuation Mach numbers $M_0 = 0.173$, 0.346, and 0.519, respectively (based on rms velocity and mean speed of sound). The initial Reynolds number Re_0 for the three cases (based on Taylor microscale and rms velocity) was 35.1. Various stages of the decay were examined, and the fraction of points with backscatter, volume-averaged subgrid-scale dissipation, and backscatter are shown in Fig. 11. The magnitude of the subgrid-scale dissi-

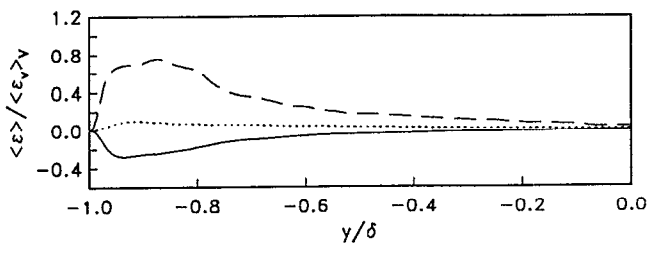

FIG. 6. Subgrid-scale dissipation normalized by $\langle\epsilon_v\rangle_V$; Re = 3300 turbulent channel flow, $\Delta_i = 4\Delta x_i$, $\alpha = 0.22$; Gaussian filter. ——: Plane-averaged dissipation $\langle\epsilon_{SGS}\rangle$; – – –: root-mean-square fluctuation of ϵ_{SGS}; ····: plane-averaged backscatter $\langle\epsilon_+\rangle$.

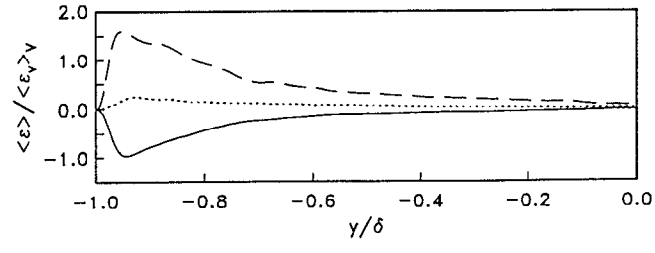

FIG. 8. Subgrid-scale dissipation normalized by $\langle\epsilon_v\rangle_V$; Re = 3300 turbulent channel flow, $\Delta_i = 4\Delta x_i$, $\alpha = 0.29$; box filter. ——: Plane-averaged dissipation $\langle\epsilon_{SGS}\rangle$; – – –: root-mean-square fluctuation of ϵ_{SGS}; ····: plane-averaged backscatter $\langle\epsilon_+\rangle$.

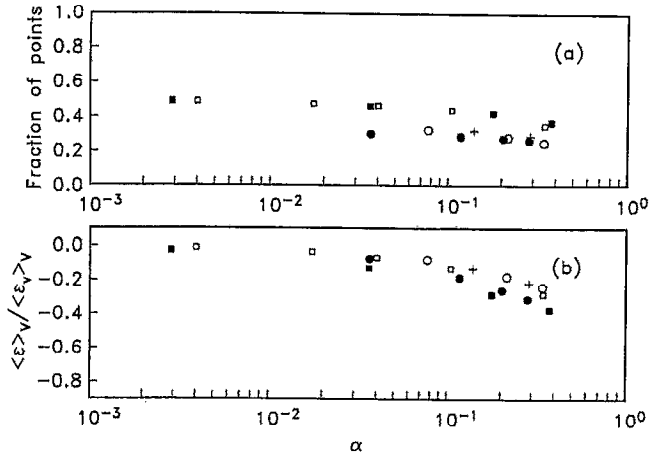

FIG. 9. Volume-averaged fraction of backscatter points and subgrid-scale dissipation. □: Re = 3300 turbulent channel flow, cutoff filter; ■: Re = 7900 turbulent channel flow, cutoff filter; ○: Re = 3300 turbulent channel flow, Gaussian filter; ●: Re = 7900 turbulent channel flow, Gaussian filter; + : Re = 3300 turbulent channel flow, box filter. (a) Fraction of backscatter points; (b) subgrid-scale dissipation.

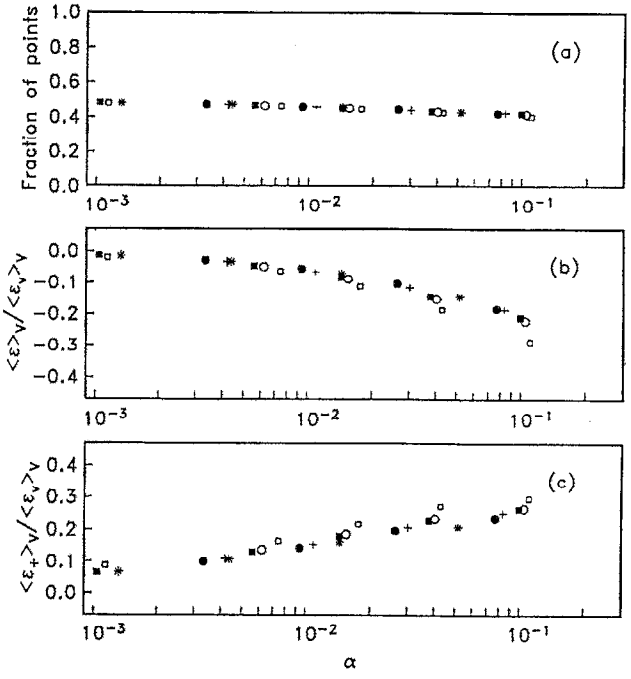

FIG. 11. Volume-averaged fraction of backscatter points, subgrid-scale dissipation and backscatter. Compressible isotropic turbulence, cutoff filter. $Re_0 = 35.1$ for all cases. □: Re = 22.5, $M = 0.132$, $M_0 = 0.173$; ○: Re = 19.8, $M = 0.113$, $M_0 = 0.173$; ■: Re = 19.4, $M = 0.220$, $M_0 = 0.346$; ●: Re = 17.3, $M = 0.182$, $M_0 = 0.346$; +: Re = 18.0, $M = 0.289$, $M_0 = 0.519$; ⋆: Re = 15.0, $M = 0.213$, $M_0 = 0.519$. (a) Fraction of backscatter points; (b) subgrid-scale dissipation; (c) subgrid-scale backscatter.

pation increases with filter width; within the range of filter widths examined, the subgrid-scale backscatter also increases with filter width, a result consistent with the turbulent channel flow. No dependence on the Mach number was observed. The increase in backscatter with Reynolds number observed above (Figs. 3 and 10) is also noticeable here.

IV. CONCLUDING REMARKS

A numerical investigation of subgrid-scale backscatter was conducted to determine the extent and magnitude of the energy transfer from small to large scales. It has been found that, when a cutoff filter is used, backscatter occurs at nearly half of the points in the flow. The mean subgrid-scale dissipation, which is usually negative, is the sum of two large quantities: energy transfer from large to small scales and backscatter. Each of these events is significantly larger than the mean SGS dissipation. Strong backward and forward scatter events are fairly well correlated with regions of high Reynolds stress in the near-wall region.

When the Gaussian filter is used the amount of backscatter decreases since part of the energy transfer between large and small scales is accounted for as an interaction between subgrid scales. The results obtained with the box filter in real space, which is implicitly applied by finite difference schemes,[2] are intermediate between those obtained with the cutoff and Gaussian filters.

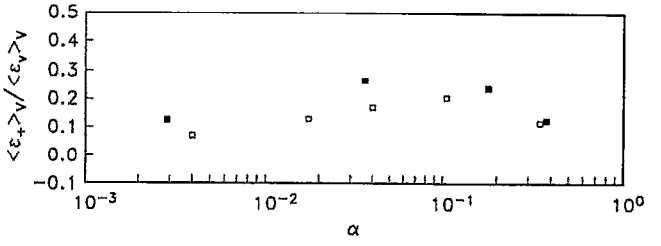

FIG. 10. Volume-averaged backscatter. □: Re = 3300 turbulent channel flow, cutoff filter; ■: Re = 7900 turbulent channel flow, cutoff filter.

While the magnitude of the SGS dissipation (normalized by the volume-averaged viscous dissipation) increases with filter width independently of Reynolds number and filter type, backscatter increases with Reynolds number both for the channel flow and for isotropic decay. Similar results were observed in compressible isotropic turbulence independently of Mach number.

The results of this work confirm and extend the findings of Ref. 5 that indicated that backscatter-generating events occur frequently. Backscatter-producing events have the effect of locally transferring energy from small to large scales, and their accurate modeling is, of course, desirable. For the transitional channel flow, inaccurate prediction of the subgrid-scale dissipation has proven to yield very inaccurate development of the perturbations, while for fully developed channel flow absolutely dissipative subgrid-scale stress models have been successful. On the basis of the present work and that of Refs. 5, 8, and 9, one can speculate that, for nonequilibrium flows, backscatter must be taken into account to ensure accurate predictions by LES.

ACKNOWLEDGMENT

Partial support for the first author (UP) was provided by the Office of Naval Research under Grant No. N00014-89-J-1531.

[1] J. Smagorinsky, Mon. Weather Rev. **91**, 99 (1963).
[2] R. S. Rogallo and P. Moin, Annu. Rev. Fluid Mech. **16**, 99 (1984).
[3] J. Bardina, J. H. Ferziger, and W. C. Reynolds, AIAA Paper No. 80-1357, 1980.
[4] K. Horiuti, Phys. Fluids A **1**, 426 (1989).
[5] U. Piomelli, T. A. Zang, C. G. Speziale, and M. Y. Hussaini, Phys. Fluids A **2**, 257 (1990).
[6] V. Yakhot and S. A. Orszag, J. Sci. Comput. **1**, 3 (1986).
[7] U. Piomelli, T. A. Zang, C. G. Speziale, and T. S. Lund, in *Instability and Transition*, edited by M. Y. Hussaini and R. G. Voigt (Springer-Verlag, New York, 1990), Vol. 2, pp. 480–496.
[8] C. E. Leith, Phys. Fluids A **2**, 297 (1990).
[9] J. R. Chasnov, Phys. Fluids A **3**, 188 (1991).
[10] M. Germano, U. Piomelli, P. Moin, and W. H. Cabot, Phys. Fluids A **3**, 1760 (1991).
[11] J. Kim, P. Moin, and R. D. Moser, J. Fluid Mech. **177**, 133 (1987).
[12] T. A. Zang, N. Gilbert, and L. Kleiser, in Ref. 7, pp. 283–299.
[13] S. Lee, S. J. Lele, and P. Moin, Phys. Fluids A **3**, 657 (1991).